OPEN ACCESS

Original research

Rare variant association analyses reveal the significant contribution of carbohydrate metabolic disturbance in severe adolescent idiopathic scoliosis

Wen Wen,[1,2] Zhengye Zhao,[1,3] Zhifa Zheng,[1,3] Sen Zhao,[1,4] Hengqiang Zhao,[1,5] Xi Cheng ,[1,2] Huakang Du,[1,2] Ziquan Li,[1,3] Shengru Wang,[1,3] Guixing Qiu,[1,3] Zhihong Wu,[1,6] Terry Jianguo Zhang,[1,3] Nan Wu [1,3,7]

► Additional supplemental material is published online only. To view, please visit the journal online (https://doi.org/10.1136/jmg-2023-109667).

For numbered affiliations see end of article.

Correspondence to
Dr Nan Wu, Department of Orthopedic Surgery, State Key Laboratory of Complex Severe and Rare Diseases, Peking Union Medical College Hospital, Peking Union Medical College and Chinese Academy of Medical Sciences; Key Laboratory of Big Data for Spinal Deformities, Chinese Academy of Medical Sciences, Wenzhou Medical University, Beijing, China; dr.wunan@pumch.cn

WW, ZZ and ZZ contributed equally.

Received 2 October 2023
Accepted 18 February 2024
Published Online First 8 May 2024

To cite: Wen W, Zhao Z, Zheng Z, *et al*. *J Med Genet* 2024;**61**:666–676.

ABSTRACT

Background Adolescent idiopathic scoliosis (AIS), the predominant genetic-influenced scoliosis, results in spinal deformities without vertebral malformations. However, the molecular aetiology of AIS remains unclear.

Methods Using genome/exome sequencing, we studied 368 patients with severe AIS (Cobb angle >40°) and 3794 controls from a Han Chinese cohort. We performed gene-based and pathway-based weighted rare variant association tests to assess the mutational burden of genes and established biological pathways. Differential expression analysis of muscle tissues from 14 patients with AIS and 15 controls was served for validation.

Results *SLC16A8*, a lactate transporter linked to retinal glucose metabolism, was identified as a novel severe AIS-associated gene (p=3.08E-06, false discovery rate=0.009). Most AIS cases with deleterious *SLC16A8* variants demonstrated early onset high myopia preceding scoliosis. Pathway-based burden test also revealed a significant enrichment in multiple carbohydrate metabolism pathways, especially galactose metabolism. Patients with deleterious variants in these genes demonstrated a significantly larger spinal curve. Genes related to catabolic processes and nutrient response showed divergent expression between AIS cases and controls, reinforcing our genomic findings.

Conclusion This study uncovers the pivotal role of genetic variants in carbohydrate metabolism in the development of AIS, unveiling new insights into its aetiology and potential treatment.

WHAT IS ALREADY KNOWN ON THIS TOPIC

⇒ Adolescent idiopathic scoliosis (AIS) is a complex trait with genetic predisposition and uncertain aetiology.

⇒ A prevalent observation of low body mass index in AIS hints at a potential contribution of metabolic factors to AIS development.

WHAT THIS STUDY ADDS

⇒ Through gene-based and pathway-based rare variant association analyses within a cohort, our study identifies the lactate transporter gene, *SLC16A8*, as a novel candidate gene for severe AIS and reveals a predominant enrichment of carbohydrate metabolism in severe AIS.

⇒ Additionally, we discerned differential expression relating to glucose metabolism and nutritional response levels in muscle tissue.

HOW THIS STUDY MIGHT AFFECT RESEARCH, PRACTICE OR POLICY

⇒ Our findings underscore the critical role of carbohydrate metabolism in severe AIS.

⇒ Early carbohydrate supplementation may potentially prevent the development of AIS, offering a novel perspective in AIS management.

INTRODUCTION

Scoliosis, characterized by a lateral curvature of the spine, represents a multifactorial disorder highly influenced by genetic factors. It may manifest as part of the phenotypic spectrum of genetic syndromes such as Marfan syndrome, spinal muscular atrophy and osteogenesis imperfecta. However, in approximately 80% of patients, scoliosis appears to be idiopathic scoliosis (IS), presenting without an identifiable underlying aetiology, with adolescent idiopathic scoliosis (AIS) forming the largest subset when classified by age of onset.[1 2] Despite the absence of vertebral malformations, IS can develop into severe spinal deformities resulting in dysmorphic feature, low back pain, incapacity to work or even paralysis if not treated.[3]

To date, the molecular aetiology of AIS remains largely unclear. Prior twin studies have estimated AIS heritability to exceed 85%,[4 5] underscoring a pronounced genetic predisposition. Genome-wide association studies (GWAS) have discovered numerous significant AIS susceptibility loci near several matrisome-related genes including *LBX1*,[6] *GPR126*,[7] *BNC2*,[8] *PAX1*,[9] *SLC39A8*[10] and *SOX9*,[11] along with other novel candidate genes[11 12] for subsequent functional validation. However, these SNPs account for only approximately 5% of AIS heritability, and the application of the polygenic risk score (PRS) merely elevates this figure to 11%,[13] suggesting the inevitable contribution of rare variants to AIS genetic architecture. Individual large familial studies have pinpointed rare variants in *HSPG2*,[14] *POC5*[15] and *CELSR2R*[16] with co-segregation patterns, as putative pathogenic variants for AIS. Rare-variant burden analyses have

demonstrated mutational enrichment of *FBN1*, *FBN2*[17] and musculoskeletal collagen genes[18] in severe AIS cases, although these results were restricted to European ancestry.

In this study, we performed next-generation sequencing (NGS) for a Han Chinese cohort with severe AIS to analyse whole exome-wide rare variants, with the objective of unveiling new elements of the 'AIS etiology puzzle'. Gene-based and pathway-based burden analyses were undertaken to identify significant genes and biological processes implicated in AIS pathogenesis.

METHODS

Study subject

Blood samples of 368 unrelated Han Chinese individuals with severe AIS (Cobb angle ≥40°, age of onset between 10 and 18 years) who underwent spinal surgery at Peking Union Medical College Hospital (PUMCH) under the Deciphering Disorders Involving Scoliosis & COmorbidities (DISCO, http://discostudy.org/) study group, from November 2016 to November 2021 for correction of scoliosis or kyphosis were consecutively recruited. The diagnosis of AIS was strictly confirmed by both an orthopaedic surgeon and a radiologist using series of clinical and radiological techniques (online supplemental methods). More clinical features of the cases are listed in online supplemental table 1.

The control individuals were aggregated from individuals who underwent exome sequencing at the Medical Research Center, PUMCH for clinical or research purposes without IS or any other skeletal malformation. The resultant control dataset constituted 3794 unrelated individuals, maintaining a balanced sex distribution.

Next-generation sequencing

NGS, including whole exome sequencing (WES) or whole genome sequencing (WGS), was performed on peripheral blood DNA samples from the study participants. The number of case and control samples that underwent WES or WGS are provided in online supplemental table 2.

WES was performed in paired-end mode on the Illumina HiSeq 2000 platform, with an average depth of coverage of 70X, while PCR-free WGS was performed on the Illumina HiSeq X-Ten or NovaSeq platform with an average depth of coverage of 35X (online supplemental methods).

Variant calling and quality control

According to Peking Union Medical College Hospital pipeline,[19 20] the raw sequencing reads were mapped to the GRCh37 human reference genome using Picard (broadinstitute.github.io/picard/) and Burrow-Wheeler Aligner (BWA).[21] To optimally preserve the genomic information, the mixed WES and WGS data were initially processed as a unified WGS dataset. Using the Sentieon's Haplotyper, the resulting variant call files (VCFs) for each sample were then converted to genomic VCFs (gVCFs) and the individual gVCFs were subsequently combined and jointly called, utilizing a population-based approach to take into account information from all samples concurrently to detect low-frequency variants that may be missed when calling independently. Single-nucleotide variants and small insertions/duplications (indels) were called using the DNA sequencing module of the Sentieon software.[22] Variant-level and sample-level quality control (QC) were performed on the joint call-set (online supplemental methods). To note, variants with a missing rate >10% across the whole cohort were filtered out, mitigating the possible biases between WES and WGS data, and ensuring a more reliable and consistent dataset for analysis.

After QC filtering, a total of 1.44 million genetic variants and 362 case samples and 3740 control samples were included for subsequent analysis.

Gene-based rare variant association analysis

We classified each variant into different mask levels (from 1 to 6) and assigned weight values (ranging from 1 to 0) to each mask level according to the variant type and bioinformatic prediction results (online supplemental methods, online supplemental table 3). The mutational burden of a given gene in each individual was assigned as the maximum weight value among all ultra-rare variants carried by the individual (if any). The ACAT package[23] was used to perform the weighted mutational burden test for each gene, with the minor allelic count threshold for each gene being included set to 5 (weight≠0). P values were adjusted for multiple testing using the Benjamini-Hochberg false discovery rate (FDR) (online supplemental methods).

Gene-set enrichment analysis for lactate transporters

Based on the gene-based analysis result, we performed enrichment analysis for six established lactate transporter genes set including proton-coupled and sodium-dependent monocarboxylates transporters (MCTs and SMCTs) based on the function and structure according to the literatures[24 25] (online supplemental table 7). We used the statistic derived from the gene-based association result and matching background genes to the specified gene set via a k-dimensional tree. A one-sided Wilcoxon test was implemented to evaluate whether the given gene set had a lower p value than expected.

Pathway-based rare variant burden analysis

We tested the aggregated mutational burden of gene sets related to biological processes, molecular pathways or disease phenotypes. The associated gene sets were retrieved from The Molecular Signatures Database (MSigDB, https://www.gsea-msigdb.org/gsea/msigdb/, accession date: 15 August 2022), collecting curated canonical pathways and ontology gene sets from diverse resources including Kyoto Encyclopedia of Genes and Genomes (KEGG, https://www.genome.jp/kegg/), Gene Ontology (GO, http://geneontology.org/) biological process, Reactome (https://reactome.org/), The Pathway Interaction Database (PID, http://pid.nci.nih.gov), BioCarta (http://www.biocarta.com/), WikiPathways (https://www.wikipathways.org/) and hierarchical terms under 'Abnormality of the skeletal system' (HP:0000924) in The Human Phenotype Ontology (HPO, https://hpo.jax.org/). All of these resources were accessed on 15 August 2022. Moreover, random gene sets were generated for permutation.

The algorithm for calculating the gene-set burden was referred to a latest study.[26] For a candidate gene set, the mutational weight (same as the gene-based test) of each gene was summed (per individual) into a burden score, which was then used to fit a logistic regression model to predict the case-control status. ORs and p values are presented as measures of enrichment in the tested gene sets. The Benjamini-Hochberg FDR procedure was used to adjust for multiple tests (online supplemental methods).

RNA sequencing and preprocessing

RNA data were obtained from muscle tissues of 14 patients with AIS from the initial cohort and another 15 patients diagnosed as congenital vertebral malformation (CVM) who also underwent corrective surgery for scoliosis at PUMCH. The gender

distribution aligns with the primary cohort and prior studies, showing a female-to-male ratio of 13:1 for AIS and 8:7 for the control group (online supplemental table 8). The patients were selected based on their diagnosis and the availability of the tissue samples.

The RNA sequencing raw reads were processed through in-house QC procedures and aligned to the human reference genome GRCh37 using the Hisat2[27] with default parameters (online supplemental methods). The gene expression levels were then quantified using the htseq-count[28] programme with Ensembl gene annotations (release 106), generating a count matrix with raw expression values.

Differential expression analysis and pathway enrichment

Differential gene expression analysis was performed on the raw count matrix of 14 patients with AIS and 15 CVM controls using the R package DESeq2.[29] We imported the count matrix data and generate dataset for differential expression analysis using 'DESeqDataSetFromHTSeqCount' function. To mitigate the impact of noise in the data, genes with <10 counts were filtered out as these genes are more likely to have unreliable expression estimates. Genes that showed more than a 1.5-fold change in expression when compared with controls, either upregulated or downregulated, were retained for further analysis. Pathway enrichment analysis was performed using the clusterProfiler (V.4.0)[30] with the predefined gene sets in GO and KEGG database. All the original p values were adjusted for multiple testing using the Benjamini-Hochberg FDR procedure. Similar analyses were performed between the AIS subgroups based on their variant carrying status to explore the integrated consequences of theses variants.

RESULTS

Gene-based rare variant analysis identifies *SLC16A8* as a novel candidate gene for severe AIS

We recruited a total of 368 patients with severe AIS, defined as a Cobb angle of ≥40° or a history of surgical treatment. Genome sequencing or exome sequencing was performed on all subjects, as well as on 3794 unrelated control samples. To increase the power of the association and decrease the possibility of latent disease in the control population, the study was limited to patients with severe AIS with an average Cobb angle of 51.6°. Cases in this cohort had a female bias of 84.5%, which aligns with previous research suggesting that the female-to-male ratio of affected individuals with severe malformation may be as high as 10:1. The study population consisted of individuals of Han Chinese ancestry with distant relatedness, as confirmed by genetic estimation (see 'Methods' section).

To investigate the role of rare genetic variants in AIS susceptibility, a weighted gene-based burden test was implemented on rare variants. The weight value assigned to each variant was determined based on its influence (see 'Methods' section).

As a result, *MOK* showed the strongest association with severe AIS compared with controls (p=8.86E-07, FDR=0.005, OR=0.90) (table 1, figure 1A). *MOK* encodes a ubiquitously expressed protein kinase of the MAPK superfamily, involved in cell growth, neuronal development and immune response. Homologous *mok*-knockout mice exhibited neurological phenotypes such as abnormal behaviour and decreased grip strength, according to the Mouse Genome Informatics database. The identification of *MOK* aligns with recent studies,[31 32] suggesting a potential role for neuronal development and function in the pathogenesis of AIS. However, all likely gene-disrupting variants identified in AIS cases fall outside the critical protein kinase domain and no MOK rare variant carrier exhibited neurological phenotype, attenuating the likelihood of MOK as a monogenic causal gene (online supplemental figure 1).

Second to the top signal, we identified *SLC16A8* as a novel candidate gene associated with severe AIS (p=3.08E-06, FDR=0.009, OR=7.42) (table 1, figure 1A). *SLC16A8* encodes a proton-coupled lactate transporter that is preferentially expressed in the retinal pigment and choroid plexus of the eye,[33] and is mildly expressed in various tissue types according to GTEx data (online supplemental figure 2). As a member of the MCT family, *SLC16A8* displays high affinity for lactate and shares common substrates with other MCTs, including pyruvate, ketone bodies acetoacetate, β-hydroxybutyrate and acetate, which can potentially regulate carbohydrate metabolism. Additionally, *SLC16A8* was implicated to be the major MCT isoform responsible for efflux of glycolytically derived lactic acid from white skeletal muscle.[34]

All the deleterious variants identified in our patients with AIS, including one nonsense variant (p.Glu231Ter), one frameshift variant (p.Arg235GlyfsTer28), one splicing variant (c.214+1G>C) and two predicted damaging missense variants (p.Gly296Asp, p.Leu134Pro), were located in the major facilitator superfamily domain, which is critical for the symport of lactate and protons (figure 1B). The bi-allelic variant in the same location (c.214+1G>C) has been reported to result in the absence of the SLC16A8 protein and cause a deficit in transepithelial lactate transport in retinal pigment epithelial cells, thereby increasing the susceptibility to macular degeneration,[35] confirming the pathogenicity of the splicing variant. Notably, within our cohort, a significant proportion (80%, 4/5) of patients harbouring deleterious *SLC16A8* variants developed myopia from an early age prior to the onset of scoliosis, with 75% of these cases classified as high myopia (exceeding 600 degrees) (table 2), indicating a putative association between *SLC16A8* and the development of both severe scoliosis and high myopia.

Furthermore, to evaluate the general contribution of lactate transport to the pathogenesis of AIS, we performed one-sided Wilcoxon test based on the gene-based burden result rank for established lactate transporter genes (see 'Methods' section). Our analysis revealed a noteworthy enrichment of rare variants in lactate transporter genes compared with the background level, as indicated by a significant p value of 0.01, provide further evidence for the potential involvement of lactate transporters in the genetic susceptibility to AIS.

Rare variants in carbohydrate metabolism pathway are enriched in severe AIS

To assess the cumulative effect of genetic variants on different genes functioning within the relevant biological pathways, we conducted a pathway-based gene-set burden analysis.

The result showed a prominent enrichment of rare variants in several pathway involved in carbohydrate metabolism, including the galactose metabolic process as the top signal (Gene Ontology Biological Process: GO:0006012, p=2.93E-05), followed by amino sugar and nucleotide sugar metabolism (KEGG pathway: map00520, p=4.04E-05), carbohydrate-derived catabolic process (GO:1901136, p=6.46E-05) and deoxyribose phosphate catabolic process (GO:0046386, p=7.06E-05), galactose catabolic process (GO:0019388, p=2.34E-04) (figure 2A, figure 2B, online supplemental table 4).

In our cohort, 48.5% of the patients with AIS (176/362) exhibited non-synonymous rare variants in 200 genes involved

Table 1 Gene-based rare variant association analysis results

Rank	Gene	Case.masks	Control.masks	P value	FDR	OR (95% CI)
1	*MOK*	9/362:2_mask1|1_mask2|3_mask3m|1_mask4m|2_mask5m	16/3740:2_mask1|1_mask2m|3_mask3m|6_mask4m|4_mask5m	8.86E-07	0.00537722	7.9 (2.54 to 24.6)
2	*SLC16A8*	7/362:3_mask1|1_mask2m|2_mask3m|1_mask5m	15/3740:1_mask1|1_mask2|2_mask2m|3_mask3m|7_mask4m|1_mask5m	3.08E-06	0.009353846	7.42 (2.45 to 22.5)
3	*OTUD4*	6/362:1_mask2|5_mask5m	6/3740:6_mask5m	3.99E-06	0.010363375	16.9 (1.58 to 182)
4	*DERA*	5/362:2_mask2|1_mask2m|1_mask3m|1_mask5m	16/3740:5_mask3m|11_mask5m	5.72E-06	0.010404332	8.87 (2.12 to 37.1)
5	*CEP170B*	9/362:1_mask1|4_mask2|1_mask4m|3_mask5m	44/3740:1_mask1|3_mask2|1_mask3m|7_mask4m|32_mask5m	6.38E-06	0.010562225	5.7 (1.97 to 16.5)
6	*ACTRT1*	5/362:1_mask1|2_mask2m|1_mask3m|1_mask4m	14/3740:3_mask3m|5_mask4m|6_mask5m	7.03E-06	0.010663846	9.9 (2.46 to 39.8)
7	*RP11-477N12.3*	6/362:3_mask1|2_mask3m|1_mask4m	17/3740:2_mask1|4_mask3m|6_mask4m|5_mask5m	9.20E-06	0.011965967	7.36 (2.28 to 23.8)
8	*MTNR1B*	3/362:1_mask2m|1_mask3m|1_mask4m	6/3740:2_mask4m|1_mask5|3_mask5m	1.02E-05	0.012327097	14.5 (1.78 to 118)
9	*C9orf116*	2/362:1_mask1|1_mask2	6/3740:6_mask5m	1.74E-05	0.018556476	21.7 (2.23 to 211)
10	*NFASC*	9/362:1_mask2|3_mask3m|1_mask4m|4_mask5m	28/3740:6_mask3m|3_mask4m|2_mask5|17_mask5m	2.52E-05	0.021565566	5.77 (1.56 to 21.4)
11	*SYPL1*	4/362:1_mask2|3_mask5m	2/3740:2_mask5m	2.88E-05	0.021565566	23.7 (1.42 to 393)
12	*FGF3*	4/362:1_mask1|2_mask4m|1_mask5m	6/3740:3_mask4m|3_mask5m	3.00E-05	0.021565566	13.4 (1.81 to 99.5)
13	*LDHD*	7/362:3_mask2|2_mask2m|1_mask3m|1_mask5m	44/3740:1_mask1|7_mask3m|13_mask4m|23_mask5m	3.06E-05	0.021565566	4.75 (1.66 to 13.6)
14	*CES1*	5/362:5_mask1	11/3740:4_mask1|1_mask2|2_mask2m|2_mask4m|2_mask5m	3.26E-05	0.021565566	7.46 (2.48 to 22.4)
15	*ZNF646*	4/362:2_mask1|1_mask3m|1_mask5m	15/3740:2_mask3m|4_mask4m|9_mask5m	3.27E-05	0.021565566	8.94 (1.95 to 41)
16	*RP11-618P17.4*	5/362:1_mask1|1_mask2m|2_mask4m|1_mask5m	11/3740:1_mask1|2_mask4m|1_mask5|7_mask5m	3.32E-05	0.021565566	10.7 (2.13 to 54.2)
17	*AKR1B15*	4/362:2_mask1|2_mask5m	3/3740:1_mask2|2_mask5m	3.61E-05	0.022628051	18.7 (2.53 to 138)
18	*GALE*	9/362:1_mask1|6_mask2m|1_mask3m|1_mask5m	31/3740:1_mask1|2_mask2|9_mask2m|7_mask3m|3_mask4m|9_mask5m	4.51E-05	0.026951593	4.63 (1.88 to 11.4)
19	*IL17RB*	3/362:2_mask1|1_mask2	4/3740:1_mask1|1_mask2|2_mask5m	5.28E-05	0.028204272	13.7 (2.64 to 71.2)
20	*KCNC2*	3/362:2_mask2|1_mask5m	6/3740:3_mask4m|3_mask5m	5.35E-05	0.028204272	13.4 (1.81 to 99.5)

The table shows the top 20 genes identified in the analysis, along with the minor allele counts and variant mask levels for each gene. OR was calculated for AIS cases versus in-house controls. The original p values were calculated using the weighted burden test and were adjusted for multiple comparisons using the Benjamini-Hochberg FDR method.
FDR, false discovery rate.

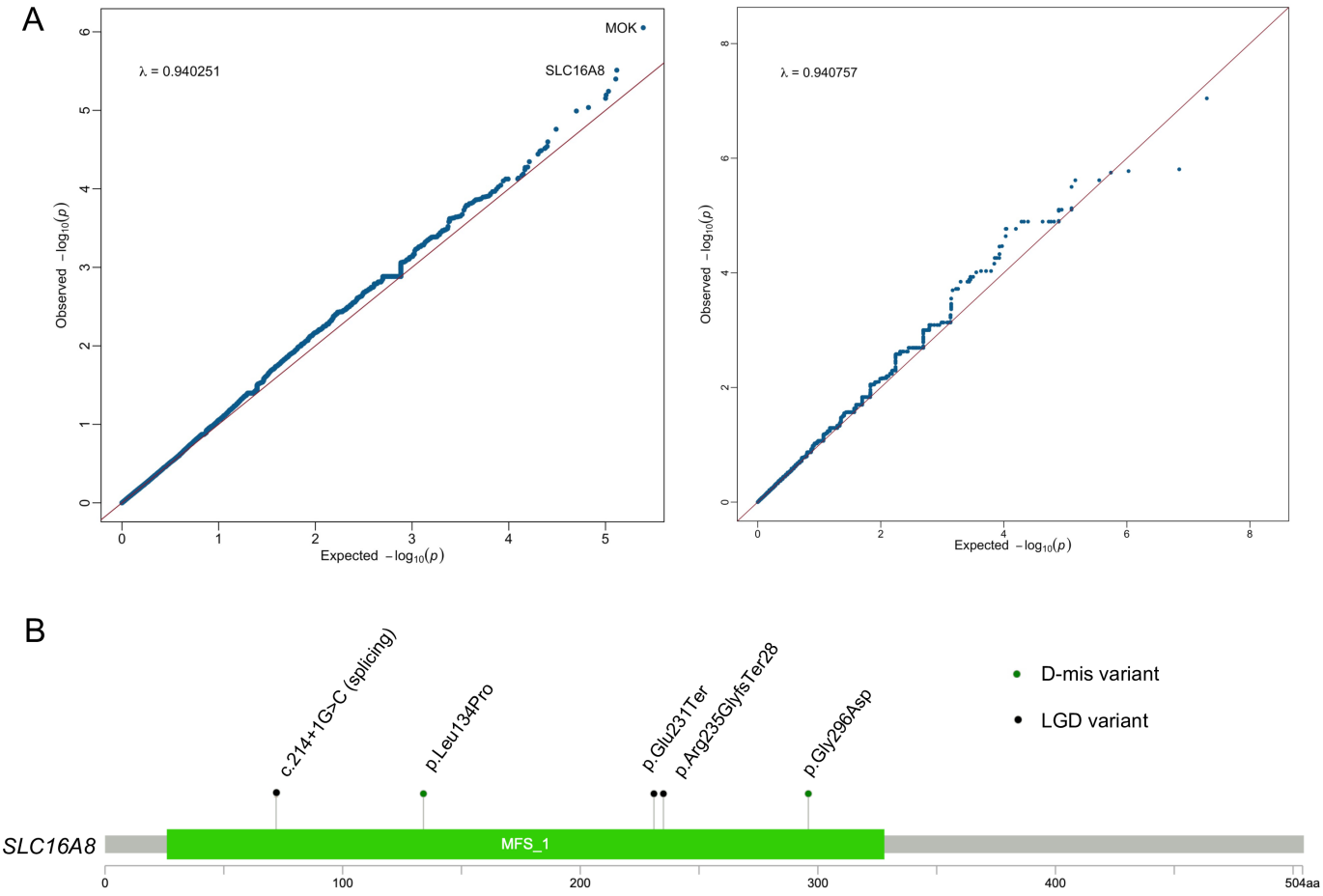

Figure 1 Gene-based rare variant association analysis identifies *SLC16A8* as a novel candidate gene for adolescent idiopathic scoliosis (AIS). (A) Quantile-quantile (Q-Q) plots of gene-based rare variant association analysis. The y-axis represents the observed data, while the x-axis represents the expected values of a normal distribution. Q-Q plots were generated for all rare non-synonymous variants (left) to identify disease-associated genes, and for synonymous variants (right) as a background control. The plotted points show the deviation of the observed distribution from the expected normal distribution. (B) Mutational spectrum of deleterious missense (D-mis) and likely gene-disrupting (LGD) variants in *SLC16A8* identified from AIS cases. MFS, major facilitator superfamily domain.

in these candidate carbohydrate metabolism pathways, a significantly higher proportion than that observed in the in-house controls (39.1%; 1466/3740) (p=1.11E-05, Fisher's exact test), with higher proportion of deleterious variants according to the mask level (figure 2C, online supplemental table 5). However, unlike the observations in *SLC16A8*, we found that variants in these carbohydrate metabolism genes mostly exhibited variants with moderate or low impact and did not show substantial loss-of-function variants (figure 2C). Meanwhile, we noted that 80.7% of the patients (142/176) carried more than one rare variant per individual (figure 2D). Additionally, the ORs of each carbohydrate metabolism pathway were also not as high as those of other significant pathways (figure 2B).

These significant pathways, which are derived from glucose metabolism, are interdependent and play crucial roles in energy supply, synthesis of glycosaminoglycans, glycosylation of proteins and lipids and generation of derivatives for cellular signalling (figure 3). Of particular significance is the galactose

Table 2 Clinical information of patients with rare deleterious variants in *SLC16A8* and corresponding variant annotation

Gender	Phenotype	Cobb angle (largest)	Myopia degree	Variant location*	Mask level	Consequence	GnomAD exome AF†
Female	High myopia, thoracic and lumbar scoliosis	50	800	chr22_38477341_CT_C	mask1	Frameshift	0
Female	High myopia, lumbar scoliosis, spondylolisthesis	60	800	chr22_38477354_C_A	mask1	Stop gained	0.00001563
Female	High myopia, hepatic hemangioma, renal hamartoma, thoracic and lumbar scoliosis, finger joint hypermobility, brown skin plaques	52	800	chr22_38478666_C_G	mask1	Splice donor loss	7.30E-05
Female	Myopia, thoracic and lumbar scoliosis	45	500	chr22_38477158_C_T	mask2m	Missense	0
Female	Thoracic scoliosis, ventricular septal defect	78	Unkown	chr22_38477644_A_G	mask3m	Missense	0

*The location is according to the GRCh37 reference.
†Frequency represents the highest frequency of all the available ancestries.
AF, allele frequency; GnomAD, Genome Aggregation Database.

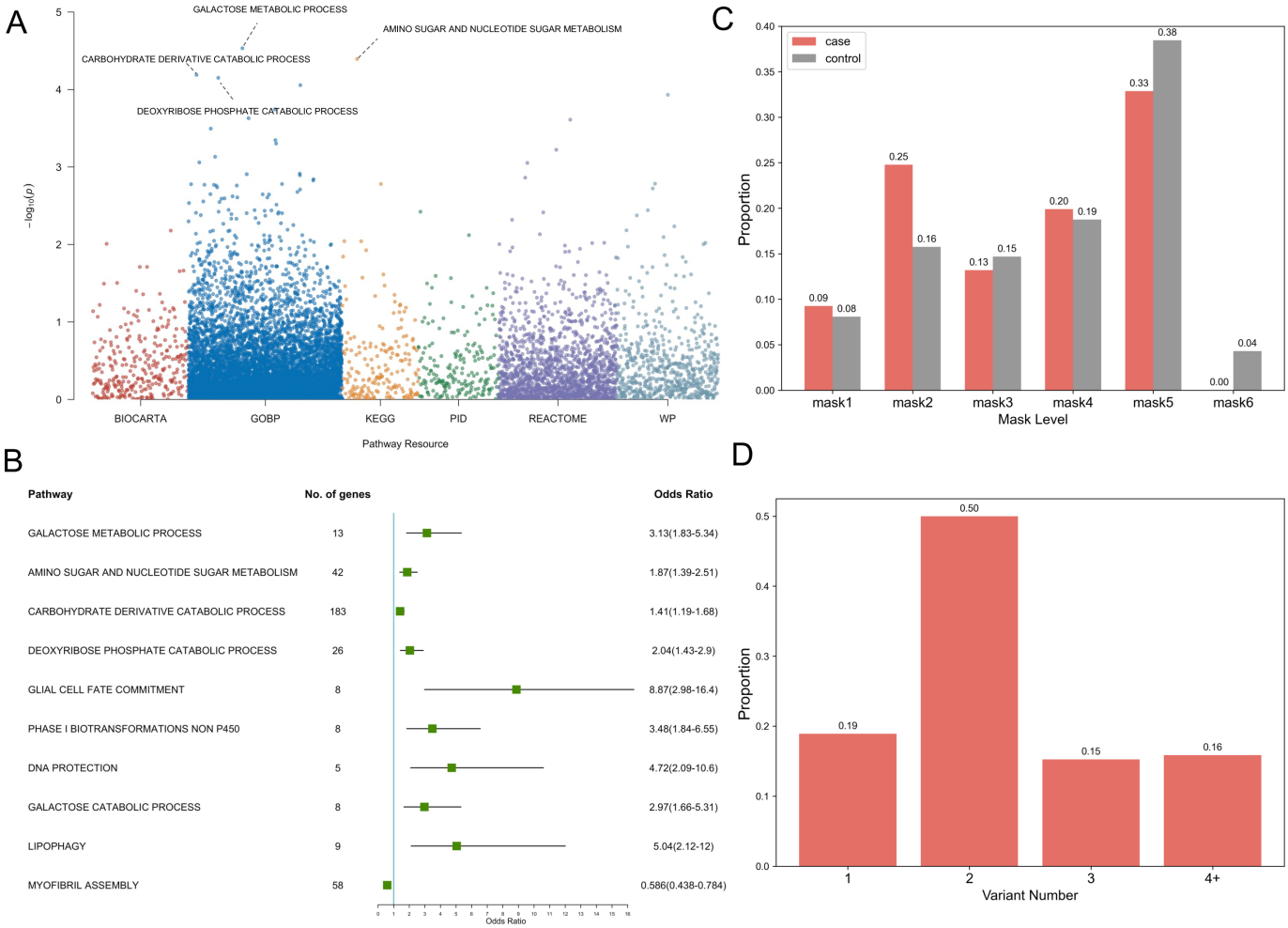

Figure 2 Pathway-based gene-set burden analysis implicates carbohydrate metabolism in the pathogenesis of adolescent idiopathic scoliosis (AIS). (A) Manhattan plot of pathway-based rare variant association. The y-axis represents the −log10 p values for pathways, while the x-axis represents their resource. The data sources selected for the analyses were BioCarta, Gene Ontology Biological Process (GOBP), Kyoto Encyclopedia of Genes and Genomes (KEGG), The Pathway Interaction Database (PID), Reactome and WikiPathways (WP). The red line indicates the threshold for statistical significance. The plot shows a peak for carbohydrate metabolism, indicating significant association of rare variants in this pathway with AIS. (B) Forest plot of the top 10 pathways of pathway-based rare variant association result. The squares represent the ORs for each pathway, with the horizontal lines representing the corresponding 95% CIs. (C) Histogram of the distribution of non-synonymous rare variants in cases (n=362) and controls (n=3740) in genes involved in carbohydrate metabolism. The proportions of variants for each variant mask level are shown above the bar. (D) Bar chart showing the distribution of patients with different variant numbers in the cases. The number of patients harbouring one, two, three or more variants are shown.

metabolic process pathway, which mainly converts galactose into glucose-6-phosphate, a form of glucose that can be used for energy production or stored as glycogen for later use. Among the different components of the galactose metabolic process, the galactose catabolic processes exhibited an independent significance and a comparative effect size (OR=2.97) (figure 2B), highlighting the possible critical role of energy supplement in the association between galactose metabolic process and AIS.

Additionally, genes critical for carbohydrate pathway function, such as *GALE*, *DERA* and *LDHD*, were also identified as being among the highest-ranking results in the gene-based burden analysis (table 1, figure 3). Dysfunction of these genes could cause imbalances in energy storage, cell growth and proliferation, developmental signalling and extracellular matrix (ECM) production and maintenance, which could potentially contribute to scoliosis development.

Differential expression analysis of muscle tissue highlights the participation of metabolism in AIS development

To validate the preliminary genomic findings and further explore the potential role of metabolism in the pathogenesis of AIS, we performed a differential expression analysis on muscles tissues obtained from 14 patients with AIS. Our choice of muscle tissue for subsequent analyses hinged on the accessibility of the tissue and the tissue-specific expression data gleaned from the Genotype-Tissue Expression project (online supplemental figure 2).

According to the genomic variant result, we divide the AIS cases into two subgroups. Five of these patients carried likely gene-disrupting variants in different carbohydrate metabolism-related genes, a trait absent in the rest of the cohort (online supplemental table 9). As a result, differentially expressed genes (DEGs) of the AIS subgroups demonstrated a consistent enrichment in glucose metabolic process (p=1.93E-04, FDR=0.12), complemented by additional enrichment in long-chain fatty

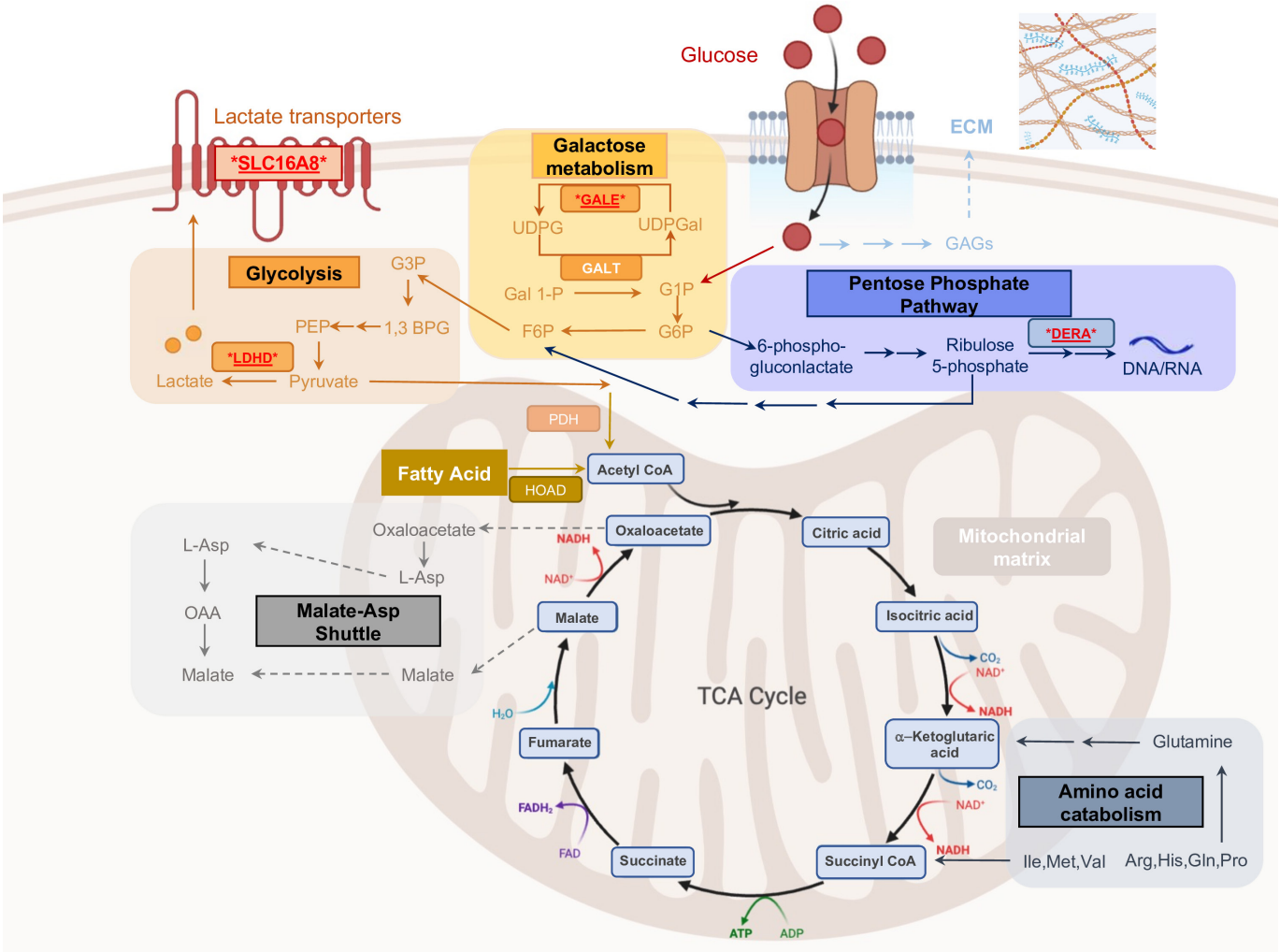

Figure 3 Illustration of the metabolic pathway of carbohydrates and pinpointed candidate genes. The figure depicts part of the carbohydrate metabolic pathway and the biological processes derived from this pathway, highlighting the enzymes and reactions involved in the breakdown of glucose and other sugars, as well as the generation of extracellular matrix (ECM). Candidate genes of top 20 nominal significance, identified through gene-based burden analysis, are emphasised by underlining and a red colour scheme. TCA, tricarboxylic acid.

acid import process (p=2.00E-04, FDR=0.12) (online supplemental figure 3 and table 10), indicating the potential of the candidate variants to disrupt carbohydrate metabolism and lipid metabolism.

As a general control, we collected muscle tissues from 15 patients diagnosed with CVM, characterised by vertebral dysplasia and/or vertebral fusion. Given the distinct vertebral anomalies observed in CVM, we hypothesised that the underlying genetic mechanisms may differ from those involved in AIS. Our analysis highlighted numerous enriched metabolic pathways among the DEGs between the AIS cases and CVM controls. Notably, there was a significant enrichment in the positive regulation of catabolic processes (p=2.95E-06, FDR=0.01) as the top signal. Aside from catabolic processes, we also discerned a noteworthy disparity in the response to nutrient levels between patients with AIS and controls (p=2.37E-05, FDR=0.02) (online supplemental figure 4 and online supplemental table 11), suggesting that patients with AIS may have heightened sensitivity to changes in nutrient availability, leading to a more vulnerable pattern in energy regulation. In terms of enriched cellular components, the mitochondrial matrix emerged with the highest significance (p=8.12E-05, FDR=0.01), which is a critical site for metabolism, including the tricarboxylic acid cycle (figure 3, online supplemental table 11).

Distinct clinical manifestation of AIS patients with rare variants in carbohydrate metabolism pathways

To determine whether patients with AIS carrying rare variants in carbohydrate metabolism pathways show distinct clinical features, we conducted a comparative analysis between patients with AIS with rare variants and without rare variants in any relevant gene. The clinical information of certain patients was missing due to lost follow-up or lack of documentation, especially the body mass index (BMI), which was omitted in each independent comparison.

Our results did not reveal any significant different clinical features between patients with AIS with rare non-synonymous variants in carbohydrate metabolism pathways and those without rare variant in relevant genes (online supplemental table 6). However, when we restricted our comparison analysis to deleterious rare variants (mask level 1–3, online supplemental table 3) in the pathways, we observed a significantly larger Cobb angle in patients with AIS with deleterious rare variants compared with those without any rare variant in the carbohydrate metabolism

pathway genes (p=0.015, one-sided two-sample t-test). Similar larger curve angle was observed in patients with rare deleterious variants in the galactose metabolism pathways (p=0.0379, one-sided two-sample t-test) (online supplemental table 6). These finding suggest that abnormal energy metabolism is associated with a high risk of progression into more severe scoliosis.

Despite the general low BMI in patients with AIS (mean: 18.8 kg/m^2, upper quartile: 16.9 kg/m^2, lower quartile: 20.04 kg/m^2), consistent to previous studies,[36] there was no significant difference in BMI between the two patient groups, except a tendency towards lower BMI in patients with AIS who carried deleterious variants in galactose metabolism pathways (p=0.12) (online supplemental table 6).

Interplay of GWAS loci and carbohydrate metabolism genes revealed the genetic complexity underlying AIS

To elucidate the interplay between carbohydrate metabolism mechanism and common variants, we further investigate the impact of previously reported AIS-associated GWAS loci.

Initially, we implemented Functional Mapping and Annotation of GWAS[37] to perform SNP-to-gene analysis including position mapping, expression quantitative trait loci (eQTL) mapping and three-dimensional chromatin interaction mapping strategies, locating 282 genes underlying all the reported significant GWAS loci (online supplemental table 12). On the 282 prioritised genes, we identified five genes, *DERA*, *GALT*, *HPSE*, *FUCA2* and *PGM3*, that are involved in distinct carbohydrate metabolism pathways, Notably, *DERA* and *GALT* are in our gene-based burden results, ranking within the top 20 (table 1), suggesting the substantial and potentially inevitable role of carbohydrate metabolism in AIS pathogenesis, mediated through both rare and common genetic variants.

Subsequently, we conducted a PRS analysis on 1663 WGS samples of our cohort using PRScise-2[38] (online supplemental methods, online supplemental table 13). Our result did not reveal a significant difference between the PRS distributions of patients with AIS and the control group (online supplemental figure 5A), consistent with the understanding that the best-performing PRS model for AIS only accounts for approximately 10% of the heritability,[13] which was anticipated an even lesser contribution in our severe AIS cases. However, a notable leftward deviation was observed in the PRS distribution of patients with AIS carrying the *SLC16A8* variants (online supplemental figure 5B), indicating the significant effect of these *SLC16A8* variants.

We additionally investigated the inheritance pattern of a patient carrying *SLC16A8* deleterious variants (p.Gly296Asp) who also exhibited an extremely high PRS score (1.6133), falling within the top 15% of the PRS distribution. The *SLC16A8* variant was validated to inherit from her father, who was unaffected by scoliosis (online supplemental figure 6). Interestingly, the PRS scores for the parents were 0.7572 and 0.6979, placing them in the bottom 15% of PRS distribution. This significant disparity in PRS scores between the affected proband and the unaffected parents provides insights into the mechanism of incomplete penetrance mediated by polygenic factors, suggesting a protective effect against AIS in individuals with lower PRS scores, even when carrying rare deleterious variants.

DISCUSSION

The genetic architecture of AIS is multifaceted and remains enigmatic, characterised by a considerable degree of locus heterogeneity and complexity. In this study, we first performed a comprehensive genetic analysis of a Han Chinese cohort with severe AIS to identify potential genetic factors underlying the development of AIS and uncovered a substantial enrichment of rare variants in carbohydrate metabolism pathways and related genes, providing novel insights into the aetiology of AIS.

The identification of *SLC16A8*, a lactate transporter gene, as a potential candidate gene associated with severe AIS is noteworthy. Remarkably, all three patients harbouring loss-of-function *SLC16A8* variants demonstrated pronounced AIS severity and exhibited high myopia preceding scoliosis onset. As *SLC16A8* is dominantly expressed in the retinal pigment epithelium, which is an extremely energy-demanding tissue,[39] a dysfunction can lead to lactate accumulation, in the consequence, a suppressed consumption of glucose,[40] which may strongly affect the regulation of ocular growth and contribute to the earlier development of myopia compared with scoliosis. Also, it has been recently elucidated that lactate can curb cartilage matrix degradation gene expression in osteoarthritic chondrocytes and stimulate matrix synthesis via HIF1A upregulation.[41] Thus, the plausible association of *SLC16A8* with both severe scoliosis and myopia underscores the potential involvement of glucose metabolism and retinal pigment and choroid in ocular growth regulation, thereby potentially accelerating myopia onset relative to scoliosis.

Furthermore, our gene-set burden analysis disclosed a significant enrichment of rare variants in lactate transporter genes and carbohydrate metabolism pathways, thereby underlining a probable correlation between carbohydrate metabolism-related biological processes and severe AIS development. Although the impact of individual variants in the carbohydrate metabolism pathway in patients with AIS is mild, the disruption is widespread across relevant genes, resulting in a generalised perturbation and a polygenic burden in broad aspects of carbohydrate-derived metabolism. Of the most significance is the galactose metabolism, which is important for energy production and the biosynthesis of glycoproteins and glycolipids. Recent research has indicated dysregulation of galactose metabolism and glycolysis pathways in progressive patients with AIS compared with non-progressive ones, with aberrant *LBX1* expression associating with AIS paraspinal muscle energy metabolic markers.[42] The severity of curvature was significantly higher in patients carrying deleterious variants in carbohydrate-derived metabolism or galactose metabolism pathways, suggesting early stage impairments in carbohydrate, especially galactose, metabolism as a possible risk factor for severe curvature development.

Supporting the involvement of metabolism in scoliosis pathogenesis, our independent differential expression analysis of muscles revealed notable differential expression in glucose metabolism as well as lipid import process between patients with AIS harbouring deleterious variants in carbohydrate metabolic pathway genes and those who do not, suggesting that these variants can potentially modulate both carbohydrate and lipid metabolism. Furthermore, the positive regulation of catabolic processes and response to nutrient levels exhibited a significant divergence in patients with AIS compared with CVM controls. Given the central role carbohydrates play as a primary nutrient, dysfunction in carbohydrate metabolism, coupled with a high sensitivity to nutrient availability changes, could induce direct or indirect serious outcomes, such as the emergence of scoliosis without vertebrate anomalies.

Previous studies have demonstrated diverse concepts and hypotheses for the pathogenesis of AIS, including axial rotational instability,[43] relative anterior spinal overgrowth and asynchronous spinal neuro-osseous growth,[44] hormonal and metabolic factors,[45] biomechanical and neuromuscular factor[46]

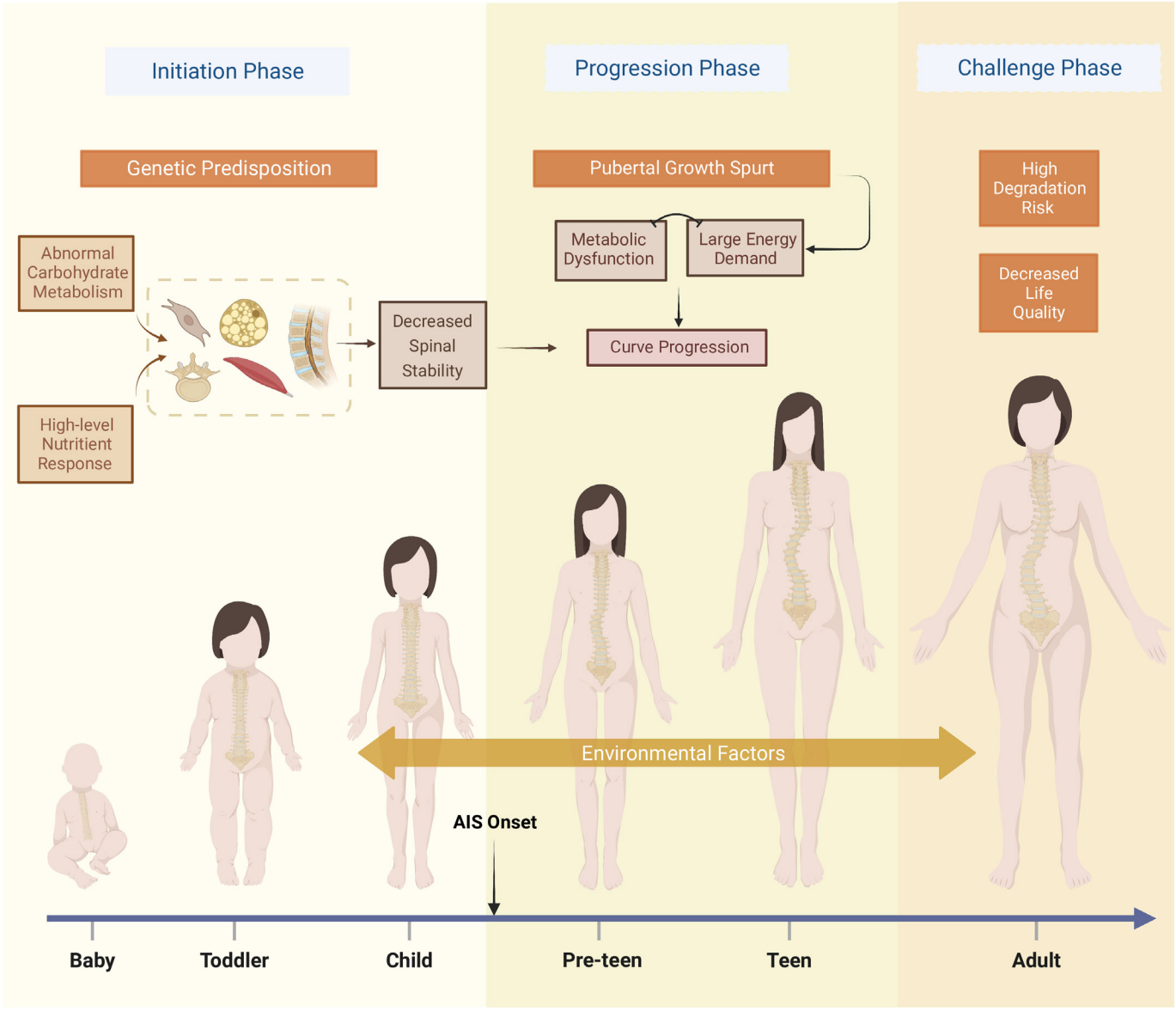

Figure 4 Illustration of carbohydrate metabolism dysfunction on severe adolescent idiopathic scoliosis (AIS) across life stages. This figure illustrates the evolution and progression of severe AIS, triggered by a generalised dysfunction in carbohydrate metabolism. The 'Initiation Phase' marks the early onset of AIS, reflecting the impact of metabolic disturbances. The 'Progression Phase' underlines the swift progression of scoliosis during periods of typical growth spurts in preteens and teens. The 'Challenge Phase' in adulthood encapsulates the enduring struggle with the disease, marked by increased risks of spinal degeneration, chronic pain, cardiopulmonary complications and diminished quality of life. Environmental factors exert influence throughout all these stages. The figure was created by BioRender.com.

and more recently, genetics factors influencing maintenance or composition of the cartilage matrisome.[47] Compared with other aspects, the understanding of the interplay between metabolic processes and AIS pathogenesis is lacking. Emerging studies have reported abnormal metabolism phenomena in patients with AIS, such as low BMI, low circulating leptin level and osteopenia.[36 48] Moreover, the inhibition of glycolysis in chondrocytic cell lines was reported to lead to hypertrophy-like changes and abnormal ECM production,[49 50] suggesting a potential role for energy metabolism in AIS development. Our findings provide a novel and comprehensive elucidation of the association between carbohydrate metabolism and AIS, suggesting that the dysregulation of metabolic processes may contribute to an elevated AIS risk, potentially via aberrant ECM production or other yet-to-be-discovered mechanisms.

In concordance with the observation that patients with AIS manifest altered body composition prior to the clinically detected scoliosis,[48] the genetic predisposition impacting carbohydrate metabolism may induce an increased spinal instability in late childhood before AIS onset. During the adolescent growth spurt, the human body experience a surge in nutrient demand, energy utilisation and biosynthesis, necessitating meticulous regulation of glucose-dependent processes. Given the exceptional flexibility of spine and the gravitational stress, an improper growth trajectory may amplify spinal instability, thereby facilitating postural instability and the onset and progression of scoliosis (figure 4). Our comparative analysis, however, did not reveal a significant metabolic manifestation, with only a slight trend towards lower BMI in patients carrying non-synonymous variants in the galactose metabolism pathway. Given the generally low BMI of

patients with AIS, a substantial metabolic disruption would be required to further decrease BMI against this already low baseline, which is not expected in our findings. Nevertheless, BMI is not an optimal or sensitive indicator of metabolic status. Future studies could employ more refined and information-rich phenotypic data, such as metabolomics, proteomics or transcriptomics of relevant cell types. An important caveat in interpreting these results is the necessity to discern whether the observed metabolic changes are primary alterations driving the disease or compensatory responses aimed at maintaining homeostasis in the face of the disease.

Author affiliations
[1]Department of Orthopedic Surgery, State Key Laboratory of Complex Severe and Rare Diseases, Peking Union Medical College Hospital, Peking Union Medical College and Chinese Academy of Medical Sciences, Beijing, Beijing, China
[2]School of Clinical Medicine, Chinese Academy of Medical Sciences and Peking Union Medical College, Beijing, Beijing, China
[3]Key Laboratory of Big Data for Spinal Deformities, Chinese Academy of Medical Sciences; Beijing, Beijing, Beijing, China
[4]Baylor College of Medicine Department of Molecular and Human Genetics, Houston, Texas, USA
[5]Feinberg School of Medicine, Northwestern University; Chicago, Chicago, Illinois, USA
[6]Medical Research Center, Peking Union Medical College Hospital, Peking Union Medical College and Chinese Academy of Medical Sciences, Beijing, Beijing, China
[7]Wenzhou Medical University, Wenzhou, Zhejiang, China

Acknowledgements We appreciate all of the patients, their families and clinical research coordinators who participated in this project. We thank the Beijing Ekitech for the technical support in database and data management. We also thank Haoxiang Xu and Jingyi He for their support in illustrating the figures.

Contributors Guarantor: NW, Clinical data gathering: ZZha, ZZhe, ZL. Methodology: WW, SZ, HZ, XC, HD. Funding acquisition: NW, JZ, ZW, SW. Project supervision: GQ, ZW, JZ. Writing—original draft: WW, SZ, ZZha, ZZhe. Writing—review and editing: NW, ZW, JZ, GQ.

Funding This research was supported by the National Key Research and Development Program of China (2023YFC2507700, 2023YFC2507701, and 2022YFC2703102), CAMS Innovation Fund for Medical Sciences (CIFMS, 2021-I2M-1-051 to JZ and NW, 2021-I2M-1-052 to ZW), National High Level Hospital Clinical Research Funding (2022-PUMCH-D-004, 2022-PUMCH-C-033), The National Natural Science Foundation of China (82072391 to NW, 81930068 and 81772299 to ZW, 81972037 and 82172382 to JZ, 81972132 to GQ), Beijing Natural Science Foundation (7191007 to ZW, 7222133 to SW).

Competing interests None declared.

Patient consent for publication Consent obtained directly from patient(s).

Ethics approval This study was approved by the Ethics Committee of the Peking Union Medical College Hospital (I-22PJ976). Participants gave informed consent to participate in the study before taking part.

Provenance and peer review Not commissioned; externally peer reviewed.

Data availability statement Data are available on reasonable request. The datasets supporting the current study have not been deposited in a public repository due to policies but are available from the corresponding author on reasonable request.

ORCID iDs
Xi Cheng http://orcid.org/0000-0001-7731-9800
Nan Wu http://orcid.org/0000-0002-9429-2889

REFERENCES

1 Choudhry MN, Ahmad Z, Verma R. Adolescent idiopathic scoliosis. *Open Orthop J* 2016;10:143–54.
2 Kikanloo SR, Tarpada SP, Cho W. Etiology of adolescent idiopathic scoliosis: a literature review. *Asian Spine J* 2019;13:519–26.
3 Vigneswaran HT, Grabel ZJ, Eberson CP, *et al*. Surgical treatment of adolescent idiopathic scoliosis in the United States from 1997 to 2012: an analysis of 20, 346 patients. *J Neurosurg Pediatr* 2015;16:322–8.
4 Inoue M, Minami S, Kitahara H, *et al*. Idiopathic scoliosis in twins studied by DNA fingerprinting: the incidence and type of scoliosis. *J Bone Joint Surg Br* 1998;80:212–7.
5 Tang NLS, Yeung H-Y, Hung VWY, *et al*. Genetic epidemiology and Heritability of AIS: a study of 415 Chinese female patients. *J Orthop Res* 2012;30:1464–9.
6 Takahashi Y, Kou I, Takahashi A, *et al*. A genome-wide association study identifies common variants near LBX1 associated with adolescent idiopathic scoliosis. *Nat Genet* 2011;43:1237–40.
7 Kou I, Takahashi Y, Johnson TA, *et al*. Genetic variants in GPR126 are associated with adolescent idiopathic scoliosis. *Nat Genet* 2013;45:676–9.
8 Ogura Y, Kou I, Miura S, *et al*. A functional SNP in BNC2 is associated with adolescent idiopathic scoliosis. *Am J Hum Genet* 2015;97:337–42.
9 Sharma S, Londono D, Eckalbar WL, *et al*. A PAX1 enhancer locus is associated with susceptibility to idiopathic scoliosis in females. *Nat Commun* 2015;6:6452.
10 Haller G, McCall K, Jenkitkasemwong S, *et al*. A missense variant in SLC39A8 is associated with severe idiopathic scoliosis. *Nat Commun* 2018;9:4171.
11 Kou I, Otomo N, Takeda K, *et al*. Genome-wide association study identifies 14 previously unreported susceptibility loci for adolescent idiopathic scoliosis in Japanese. *Nat Commun* 2019;10:3685.
12 Zhu Z, Tang N-S, Xu L, *et al*. Genome-wide association study identifies new susceptibility loci for adolescent idiopathic scoliosis in Chinese girls. *Nat Commun* 2015;6:8355.
13 Otomo N, Lu H-F, Koido M, *et al*. Polygenic risk score of adolescent idiopathic scoliosis for potential clinical use. *J Bone Miner Res* 2021;36:1481–91.
14 Baschal EE, Wethey CI, Swindle K, *et al*. Exome sequencing identifies a rare HSPG2 variant associated with familial idiopathic scoliosis. *G3 (Bethesda)* 2015;5:167–74.
15 Patten SA, Margaritte-Jeannin P, Bernard J-C, *et al*. Functional variants of POC5 identified in patients with idiopathic scoliosis. *J Clin Invest* 2015;125:1124–8.
16 Einarsdottir E, Grauers A, Wang J, *et al*. CELSR2 is a candidate susceptibility gene in idiopathic scoliosis. *PLoS One* 2017;12:e0189591.
17 Buchan JG, Alvarado DM, Haller GE, *et al*. Rare variants in FBN1 and FBN2 are associated with severe adolescent idiopathic scoliosis. *Hum Mol Genet* 2014;23:5271–82.
18 Haller G, Alvarado D, Mccall K, *et al*. A polygenic burden of rare variants across extracellular matrix genes among individuals with adolescent idiopathic scoliosis. *Hum Mol Genet* 2016;25:202–9.
19 Chen N, Zhao S, Jolly A, *et al*. Perturbations of genes essential for müllerian duct and wölffian duct development in mayer-rokitansky-küster-hauser syndrome. *Am J Hum Genet* 2021;108:337–45.
20 Zhao S, Zhang Y, Chen W, *et al*. Diagnostic yield and clinical impact of exome sequencing in early-onset scoliosis (EOS). *J Med Genet* 2021;58:41–7.
21 Li H, Durbin R. Fast and accurate short read alignment with burrows-wheeler transform. *Bioinformatics* 2009;25:1754–60.
22 Aldana R, Freed D. Data processing and Germline variant calling with the sentieon pipeline. *Methods Mol Biol* 2022;2493:1–19.
23 Liu Y, Chen S, Li Z, *et al*. ACAT: a fast and powerful P value combination method for rare-variant analysis in sequencing studies. *Am J Hum Genet* 2019;104:410–21.
24 Ganapathy V, Thangaraju M, Gopal E, *et al*. Sodium-coupled monocarboxylate transporters in normal tissues and in cancer. *AAPS J* 2008;10:193–9.
25 Felmlee MA, Jones RS, Rodriguez-Cruz V, *et al*. Monocarboxylate transporters (SLC16): function, regulation, and role in health and disease. *Pharmacol Rev* 2020;72:466–85.
26 Koko M, Krause R, Sander T, *et al*. Distinct gene-set burden patterns underlie common generalized and focal epilepsies. *EBioMedicine* 2021;72:103588.
27 Kim D, Langmead B, Salzberg SL. HISAT: a fast spliced Aligner with low memory requirements. *Nat Methods* 2015;12:357–60.
28 Anders S, Pyl PT, Huber W. HTSeq—a python framework to work with high-throughput sequencing data. *Bioinformatics* 2015;31:166–9.
29 Love MI, Huber W, Anders S. Moderated estimation of fold change and dispersion for RNA-Seq data with DESeq2. *Genome Biol* 2014;15:550.
30 Wu T, Hu E, Xu S, *et al*. clusterProfiler 4.0: a universal enrichment tool for interpreting omics data. *Innovation (Camb)* 2021;2:100141.
31 Burwell RG, Freeman BJC, Dangerfield PH, *et al*. Etiologic theories of idiopathic scoliosis: neurodevelopmental concept of maturational delay of the CNS body schema ("body-in-the-brain"). *Stud Health Technol Inform* 2006;123:72–9.

32 Formaggio E, Bertuccelli M, Rubega M, *et al*. Brain oscillatory activity in adolescent idiopathic scoliosis. *Sci Rep* 2022;12:17266.
33 Payen VL, Mina E, Van Hée VF, *et al*. Monocarboxylate transporters in cancer. *Mol Metab* 2020;33:48–66.
34 Wilson MC, Jackson VN, Heddle C, *et al*. Lactic acid efflux from white Skeletal muscle is catalyzed by the monocarboxylate transporter Isoform MCT3. *J Biol Chem* 1998;273:15920–6.
35 Klipfel L, Cordonnier M, Thiébault L, *et al*. A splice variant in SLC16A8 gene leads to lactate transport deficit in human iPS cell-derived retinal pigment epithelial cells. *Cells* 2021;10:179.
36 Ramírez M, Martínez-Llorens J, Sanchez JF, *et al*. Body composition in adolescent idiopathic scoliosis. *Eur Spine J* 2013;22:324–9.
37 Watanabe K, Taskesen E, van Bochoven A, *et al*. Functional mapping and annotation of genetic associations with FUMA. *Nat Commun* 2017;8:1826.
38 Choi SW, O'Reilly PF. Prsice-2: polygenic risk score software for biobank-scale data. *Gigascience* 2019;8:giz082.
39 Pan WW, Wubben TJ, Besirli CG. Photoreceptor metabolic reprogramming: current understanding and therapeutic implications. *Commun Biol* 2021;4:245.
40 Kanow MA, Giarmarco MM, Jankowski CS, *et al*. Biochemical adaptations of the retina and retinal pigment epithelium support a metabolic ecosystem in the vertebrate eye. *Elife* 2017;6:e28899.
41 Zhang X, Wu Y, Pan Z, *et al*. The effects of lactate and acid on articular chondrocytes function: implications for polymeric cartilage scaffold design. *Acta Biomater* 2016;42:329–40.
42 Wang Y, Li M, Chan C-O, *et al*. Biological effect of dysregulated LBX1 on adolescent idiopathic scoliosis through modulating muscle carbohydrate metabolism. *Spine J* 2022;22:1551–65.
43 Wong C. Mechanism of right thoracic adolescent idiopathic scoliosis at risk for progression; a unifying pathway of development by normal growth and imbalance. *Scoliosis* 2015;10:2.
44 Chu WC, Lam WM, Ng BK, *et al*. Relative shortening and functional tethering of spinal cord in adolescent scoliosis–result of asynchronous neuro-osseous growth, summary of an electronic focus group debate of the IBSE. *Scoliosis* 2008;3:8:1–24:.
45 Lombardi G, Akoume M-Y, Colombini A, *et al*. Biochemistry of adolescent idiopathic scoliosis. *Adv Clin Chem* 2011;54:165–82.
46 Veldhuizen AG, Wever DJ, Webb PJ. The aetiology of idiopathic scoliosis: biomechanical and neuromuscular factors. *Eur Spine J* 2000;9:178–84.
47 Wise CA, Sepich D, Ushiki A, *et al*. The cartilage matrisome in adolescent idiopathic scoliosis. *Bone Res* 2020;8:13.
48 Clark EM, Taylor HJ, Harding I, *et al*. Association between components of body composition and scoliosis: a prospective cohort study reporting differences identifiable before the onset of scoliosis. *J Bone Miner Res* 2014;29:1729–36.
49 Nishida T, Kubota S, Aoyama E, *et al*. Impaired glycolytic metabolism causes chondrocyte hypertrophy-like changes via promotion of phospho-Smad1/5/8 translocation into nucleus. *Osteoarthritis Cartilage* 2013;21:700–9.
50 Hollander JM, Zeng L. The emerging role of glucose metabolism in cartilage development. *Curr Osteoporos Rep* 2019;17:59–69.